2026 European Conference on Computing in Construction
Corfu, Greece
July 12-15, 2026

A DECENTRALIZED DIGITAL TWINNING APPROACH FOR ASSESSING CIVIL ENGINEERING STRUCTURES

Kosmas Dragos, Thamer Al-Zuriqat, and Kay Smarsly
Institute of Digital and Autonomous Technology, Hamburg University of Technology, Blohmstraße 15, 21079 Hamburg, Germany

Abstract

In wireless structural health monitoring (SHM), the focus is usually placed on reducing the power-consuming data transmission for preserving the limited resources of wireless sensor nodes. In this direction, embedded computing has been leveraged for distributing SHM data analysis tasks to the sensor nodes instead of transmitting raw data to centralized servers. This paper reports on decentralizing SHM tasks using reduced-order numerical models of structures, embedded into wireless sensor nodes as decentralized digital twins that use sensor data to assess the structural condition. The applicability of the proposed approach is demonstrated via laboratory validation tests.

Introduction

The traction that wireless structural health monitoring (SHM) has been gaining in structural maintenance since the end of the 20th century has mainly been attributed to the drawbacks of cable-based technologies for SHM, in terms of labor installation and cabling (Çelebi, 2002). Notwithstanding the significant benefits of wireless technologies, non-negligible drawbacks have been recognized already from early wireless SHM approaches, related to low transmission reliability and limited power autonomy (Lynch and Loh, 2006). The recent growing trends towards digitalization, fostering state-of-the-art technological concepts, such as Internet-of-Things systems (Al-Zuriqat et al., 2025), has brought wireless SHM once again to the forefront, frequently placed within the framework of emerging computing paradigms, such as embedded systems design and edge computing (Buckley et al., 2021).

Considerable research effort has been invested in tackling the weakest point of wireless SHM systems: The reliance on batteries, which limits the power autonomy. In this direction, the main schools of thought have focused on either integrating hardware components capable of generating power or reducing in-network wireless transmission both among wireless sensor nodes and between wireless sensor nodes and centralized servers. The former school of thought promotes the installation of energy harvesters for converting energy from ambient sources (solar, wind) to power, or – in some cases – exploiting the very vibration of structures for charging wireless sensor nodes (Park et al., 2008). Nevertheless, energy harvesting does not impose fundamental changes in the design and operation of wireless SHM systems. The latter school of thought builds upon embedded (or edge) computing, which aims to convert wireless sensor nodes from mere data collection devices to quasi-independent platforms capable of autonomously executing SHM tasks (Dragos and Smarsly, 2015). In this context, embedded/edge computing effects a decisive change on the design of wireless SHM systems, as well as on the overall SHM strategies.

Embedded computing in wireless SHM has been studied extensively over the last three decades. Seminal work proving the superiority of embedded computing in SHM over centralized approaches, in terms of energy efficiency, dates back to the beginning of the millennium with the works of Mitchel et al. (2000), Spencer Jr. et al. (2003), Lynch et al. (2004) and Wang et al. (2007), paving the way for introducing a plethora of embedded computing approaches, mostly from 2008 onwards. Common ground among most embedded computing approaches has been the extraction of features from sensor data (e.g. structural response data or environmental data) indicative of a “system state” (essentially, structural condition), which enables either identifying structural parameters or detecting structural damage. Examples include the extraction and tracking of modal parameters, reported by Zimmerman et al. (2008), the estimation of the damage location vector, introduced by Nagayama et al. (2009), and the computation of the transmissibility function between mobile sensor nodes, presented by Yi et al. (2010). In recent work, Quqa et al. (2021) have applied embedded damage detection based on the interpolation error when approximating deflection shapes using smooth functions. Other approaches for extracting features from sensor data have been based on the random decrement method (Friedmann et al., 2010), auto-regressive modeling (Kijewski-Correa and Su, 2009), and on cable-force estimation (Spencer Jr. and Cho, 2011). A special class of embedded computing approaches for wireless SHM has centered around machine learning, employed for system identification (Peckens et al., 2011), damage detection (Avci et al., 2018) and for fault diagnosis in the time domain (Smarsly and Law, 2014), in the frequency domain (Dragos et al., 2016) and in the coupled time-frequency domain (Fritz et al., 2022). Finally, embedded computing has been leveraged for eliminating synchronization errors, as part of on-board estimation of modal parameters (Dragos et al., 2018).

The literature review on embedded computing for wireless SHM reveals a trend in adopting data-driven analysis methods for on-board computations. However informative, data-driven analysis methods exhibit inherently limited information potential, due to only implicitly considering the physics dominating the structural behavior. In other words, the outcomes of data-driven analysis methods are essentially mathematical quantities, whose physical meaning cannot always be guaranteed. In this context, this paper reports on an embedded computing approach aiming to render on-board analysis "physics-informed". In particular, drawing from the state-of-the-art paradigm of digital twinning, the proposed approach focuses on decentralizing digital twins in an attempt to enable wireless sensor nodes to conduct complex SHM tasks on board with enhanced decision-making capabilities. Preliminary work on employing physics-based modeling for embedded computing has been conducted by the authors (Dragos and Smarsly, 2017; Dragos and Smarsly, 2024). Capitalizing on the preliminary work, the decentralized digital twinning approach builds upon embedding physics-based models that are computationally manageable and amenable to independent analysis on each wireless sensor node. The proposed approach is validated in laboratory tests on a shear-frame structure, demonstrating the capabilities of the decentralized digital twins in identifying structural damage.

The remainder of the paper starts with a description of the decentralized digital twinning approach, followed by the implementation and the laboratory validation test. The paper ends with the summary and conclusions, as well as with a brief discussion on potential future research.

Decentralized digital twinning

The decentralized digital twinning approach is presented in this section. First, the two steps towards producing physics-based models suitable for embedment into wireless sensor nodes (model-order reduction and model segmentation) are illuminated. Next, the overview of the approach is described.

Model-order reduction

The limited computational resources of wireless sensor nodes render the embedment of physics-based models, frequently used in structural engineering (mostly, finite element models), prohibitive. In an attempt to alleviate the computational burden of finite element (FE) models, model-order reduction (MOR) is employed. In civil engineering, the reduction usually involves representing physical structures through features, capable of capturing the structural behavior. The features are estimated either by transforming elaborate FE models, e.g., from the physical domain to the modal domain (representing a physical structure via its modal parameters) or by transforming structural response data, collected from a physical structure, from the time domain to the frequency domain (representing the structural behavior in terms of dominant frequency components, instead of raw structural response data). However, most MOR methods are associated with transforms that result in reduced-order models hardly representable in physical-coordinate systems. Consequently, coupling such reduced-order models with structural response data, corresponding to degrees of freedom with physical coordinates, is challenging.

To tackle the aforementioned challenge, the decentralized digital twinning approach, presented in this paper, employs a MOR method that partially retains representability in physical coordinates. Specifically, the dynamic condensation method is applied, which has been widely used in case studies of component mode synthesis (Bathe and Dong, 2014). Considering a physical structure, represented by a FE model of N degrees of freedom, the starting point for the dynamic condensation is the formulation of the equation of motion as follows:

$$\mathbf{M}^{N\times N}\ddot{\mathbf{x}}^{N\times 1}(t)+\mathbf{C}^{N\times N}\dot{\mathbf{x}}^{N\times 1}(t)+\mathbf{K}^{N\times N}\mathbf{x}^{N\times 1}(t)=\mathbf{p}^{N\times 1}(t). \quad (1)$$

The quantities $\mathbf{M}$, $\mathbf{C}$ and $\mathbf{K}$, represent the mass, damping, and stiffness matrices, respectively. The vectors $\ddot{\mathbf{x}}$, $\dot{\mathbf{x}}$ and $\mathbf{x}$, hold the acceleration, velocity, and displacement response data, the variable t denotes time, and $\mathbf{p}$ is the load vector. The N degrees of freedom are partitioned into two sets, the "retained" (r set) and the "condensed" (c set) degrees of freedom. Since the goal of MOR is to produce reduced-order models intuitive for SHM, the r set contains degrees of freedom measured by the SHM system, and the c set contains the rest of the degrees of freedom of the FE model. Thereupon, each of the matrices $\mathbf{A}$ in Equation 1 (with $\mathbf{A} = \{\mathbf{M}, \mathbf{C}, \mathbf{K}\}$) and each of the vectors $\mathbf{a}$ (with $\mathbf{a} = \{\ddot{\mathbf{x}}, \dot{\mathbf{x}}, \mathbf{x}\}$) are rearranged as shown below:

$$\mathbf{A}=\left[\begin{array}{c|c}\mathbf{A}_{cc} & \mathbf{A}_{cr}\\ \hline \mathbf{A}_{rc} & \mathbf{A}_{rr}\end{array}\right] \quad \mathbf{a}=\left\{\begin{array}{c}\mathbf{a}_{c}\\ \hline \mathbf{a}_{r}\end{array}\right\}. \quad (2)$$

Next, the submatrices of the c set are used for computing (i) the static-constraint modes $\mathbf{\Psi}_{cr} = (-\mathbf{K}_{cc})^{-1}\mathbf{K}_{cr}\mathbf{I}_{rr}$ and (ii) the eigenmodes $\mathbf{\Phi}_{cv} = [\boldsymbol{\varphi}_{cj}]$ ($j = 1...v$) of the eigenproblem $\mathbf{K}_{cc}\boldsymbol{\varphi}_{cj} = \lambda_j\mathbf{M}_{cc}\boldsymbol{\varphi}_{cj}$, which together form the following transformation matrix $\mathbf{\Psi}_r$:

$$\mathbf{\Psi}_r=\begin{bmatrix}\mathbf{\Phi}_{cv} & \mathbf{\Psi}_{cr}\\ \mathbf{0}_{rv} & \mathbf{I}_{rr}\end{bmatrix}. \quad (3)$$

Finally, the transformation matrix is used for computing the reduced-order r×r model matrices, $\mathbf{K}_{red}$ and $\mathbf{M}_{red}$, as shown in Equation 4.

$$\mathbf{K}_{red}=\mathbf{\Psi}_r^T\mathbf{K}\mathbf{\Psi}_r \qquad \mathbf{M}_{red}=\mathbf{\Psi}_r^T\mathbf{M}\mathbf{\Psi}_r \quad (4)$$

As regards the damping matrix, due to the generally low vibration excitation of typical SHM applications, the Rayleigh-damping approximation is adopted, which is frequently applied in civil engineering. As a result, the damping matrix is considered proportional to the stiffness matrix ($\mathbf{C}_{red} = \beta\mathbf{K}_{red}$) with β representing the Rayleigh coefficient. Proportionality with the mass matrix, also applied in civil engineering, is not considered, in this case, for simplicity. Upon completing MOR, the reduced-order model is segmented to enable its use on board the wireless sensor nodes, as will be shown in the next subsection.

Model segmentation

The dynamic condensation produces matrices of the following layout:

$$\mathbf{M}_{red} = \left[\begin{array}{c|c} \mathbf{M}_{rr} & \mathbf{M}_{rv} \\ \hline \mathbf{M}_{vr} & \mathbf{I}_{vv} \end{array}\right], \quad \mathbf{K}_{red} = \left[\begin{array}{c|c} \mathbf{K}_{rr} & \mathbf{0}_{rv} \\ \hline \mathbf{0}_{vr} & \mathbf{\Lambda}_{vv} \end{array}\right]. \quad (5)$$

In Equation 5, $\mathbf{I}$ is the unitary matrix, $\mathbf{0}$ is a zero matrix, and $\mathbf{\Lambda}$ is a diagonal matrix holding the v eigenvalues from the eigenproblem, previously shown. Moreover, the vectors assume the form $\mathbf{x}_{red} = [\mathbf{x}_c, \mathbf{q}_v]^T$, where $\mathbf{q}$ is the vector of the generalized coordinates, corresponding to the v eigenvalues. By substituting the matrices and vectors of the reduced-order model into Equation 1 and by recasting the matrix-form equation as a set of two equations, the following formulation is obtained:

$$\begin{aligned} \mathbf{M}_{rr}\ddot{\mathbf{x}}_r + \mathbf{M}_{rv}\ddot{\mathbf{q}}_v + \mathbf{K}_{rr}\left(\mathbf{x}_r + \beta\dot{\mathbf{x}}_r\right) = \mathbf{p}_r \\ \mathbf{M}_{vr}\ddot{\mathbf{x}}_r + \ddot{\mathbf{q}}_v + \mathbf{\Lambda}_{vv}\left(\mathbf{q}_v + \beta\dot{\mathbf{q}}_v\right) = \mathbf{p}_v \end{aligned} \quad (6)$$

Since the top equation contains structural response data from the r set of degrees of freedom, this equation forms the basis for the rest of the computations. The first step towards model segmentation involves eliminating terms from the equation that are unknown. For example, in typical vibration-based SHM practices, acceleration response data is collected, while measuring velocities and displacements is relatively rare. Furthermore, estimating velocities and displacements via double integration is hardly accurate, due to the inevitable contamination of acceleration response data with noise and measurement errors. To remove the "unknown" velocities and displacements, the top part of Equation 6 is transformed into the frequency domain via the fast Fourier transform (FFT):

$$\mathbf{M}_{rr}\ddot{\mathbf{X}}_r + \mathbf{M}_{rv}\ddot{\mathbf{Q}}_v + \mathbf{K}_{rr}\left(\mathbf{X}_r + \beta\dot{\mathbf{X}}_r\right) = \mathbf{P}_r. \quad (6)$$

The FFT representations of acceleration, velocity and displacement response data are denoted as $\ddot{\mathbf{X}}$, $\dot{\mathbf{X}}$, and $\mathbf{X}$, respectively. The following equivalences between the FFT representations for each frequency component f, with respect to the natural frequency ω ($\omega = 2\pi f$), are considered:

$$\dot{\mathbf{X}}_r = \frac{\ddot{\mathbf{X}}_r}{\omega \mathrm{i}} + \varepsilon_1, \qquad \mathbf{X}_r = -\frac{\ddot{\mathbf{X}}_r}{\omega^2} + \varepsilon_2. \quad (7)$$

In Equation 7, ε_1 and ε_2 are error functions of the natural frequency, accounting for the inaccuracies stemming from the approximative character of the FFT and the effects of incomplete sampling, spectral leakage, and noise. Using Equation 7, Equation 6 is converted as follows:

$$\left[\mathbf{M}_{rr} + \left(\frac{\beta}{\omega \mathrm{i}} - \frac{1}{\omega^2}\right)\mathbf{K}_{rr}\right]\ddot{\mathbf{X}}_r = \mathbf{P}_r. \quad (8)$$

Representing an extension to the approach presented in Dragos and Smarsly (2024), MOR in this paper is applied in a pair-wise manner, i.e. in pairs of degrees of freedom, corresponding to locations measured by the SHM system, designating a "master" (w) and a "slave" (o) degree of freedom (DOF) in each pair (r = 2). The purpose of applying pair-wise MOR is to produce reduced-order models as lightweight as possible, while minimizing in-network communication. In fact, each reduced-order model is designed to be embedded into the wireless sensor node measuring the master DOF, and use the model with locally collected acceleration response data, as well as with data collected from the slave-DOF (typically, neighboring) sensor node. As a result, the matrices $\mathbf{M}_{rr}$ and $\mathbf{K}_{rr}$ are 2×2 with the layout shown below:

$$\mathbf{M}_{rr} = \left[\begin{array}{c|c} m_{ww} & m_{wo} \\ \hline m_{ow} & m_{oo} \end{array}\right], \quad \mathbf{K}_{rr} = \left[\begin{array}{c|c} k_{ww} & k_{wo} \\ \hline k_{ow} & k_{oo} \end{array}\right]. \quad (9)$$

By substituting the expressions of Equation 9 into Equation 6, and by performing some mathematical manipulations, the top part of the 2×2 matrix-form equation of motion assumes the following form:

$$\begin{aligned} a_{ww} \cdot \ddot{X}_w + a_{wo} \cdot \ddot{X}_o = h_w \\ a_{ij} = \left[m_{ij} + \left(\frac{\beta}{\omega \mathrm{i}} - \frac{1}{\omega^2}\right)k_{ij}\right]. \end{aligned} \quad (10)$$

In Equation 10, h_w denotes an error term, including the quantities: $h_w = P_{\mathrm{w}} - (\mathbf{m}_{wv})^T\, \ddot{\mathbf{Q}}_v - (\beta\varepsilon_1 + \varepsilon_2)\cdot(k_{ww} + k_{wo})$. Each wireless sensor node is assigned the task to use the reduced-order model and locally collected acceleration response data $\ddot{X}_w$ to estimate the slave-DOF acceleration response data ($\ddot{X}_o$), by solving Equation 10 as:

$$\ddot{X}_o = \frac{h_w - \left[m_{ww} + \left(\frac{\beta}{\omega \mathrm{i}} - \frac{1}{\omega^2}\right)k_{ww}\right]\cdot \ddot{X}_w}{\left[m_{wo} + \left(\frac{\beta}{\omega \mathrm{i}} - \frac{1}{\omega^2}\right)k_{wo}\right]}. \quad (11)$$

Equation 11 represents a "segmented" reduced-order model, capable of being implemented into an independently operating wireless sensor node.

Following up on the previous discussion, the decentralized digital twinning approach is summarized in Figure 1. The starting point for applying the approach on each wireless sensor node involves the formulation, calibration and dynamic condensation (to master-slave DOF pairs) of a FE model representing the initial condition of the structure being monitored ("undamaged" structure). The calibration is achieved using preliminary acceleration response data from all degrees of freedom measured and by applying FE model updating. Then, a family of L FE model variants, corresponding to damage scenarios, are created by perturbing a set of structural parameters $\boldsymbol{\theta}$ and reduced, following the same condensation as in the undamaged structure. Finally, using newly collected acceleration response data, Equation 11 is applied for several FE model variants.

The error term h_w in Equation 11 is generally unknown, hindering the estimation of the slave-DOF responses. To overcome the computation difficulty, the term h_w is assumed to be random Gaussian, the acceleration response data is segmented into n time windows, and Equation 11 is applied to each time window separately to statistically limit the effect of the term h_w. As a result, a vector of slave-DOF response estimates is obtained

$\tilde{\mathbf{X}}_o = [\tilde{X}_{o1}, \tilde{X}_{o2}, ..., \tilde{X}_{on}]^T$ deviating from the respective acceleration response data $\ddot{\mathbf{X}}_o = [\ddot{X}_{o1}, \ddot{X}_{o2},..., \ddot{X}_{on}]^T$ by the error terms $\mathbf{h}_w = [h_{w1}, h_{w2},...,h_{wn}]$. The fitness of each model variant is determined upon the proximity between the vector $\tilde{\mathbf{X}}_o$ to the vector $\ddot{\mathbf{X}}_o$, computed by the coefficient of determination R^2, shown below, summed over a range Ω of frequency components, separately for the real and imaginary parts of the complex-valued $\tilde{\mathbf{X}}_o$ and $\ddot{\mathbf{X}}_o$:

$$R^2 = 1 - \frac{\sum_{j=1}^{n} \left(\ddot{X}_o - \tilde{X}_o \right)^2}{\sum_{j=1}^{n} \left(\ddot{X}_o - \bar{X}_o \right)^2}. \qquad (12)$$

In Equation 12, $\bar{X}_o$ is the mean slave-DOF response from the vector $\ddot{\mathbf{X}}_o$. The decentralized digital twinning approach is implemented in a prototype wireless SHM system and validated in a laboratory test, presented in the next section.

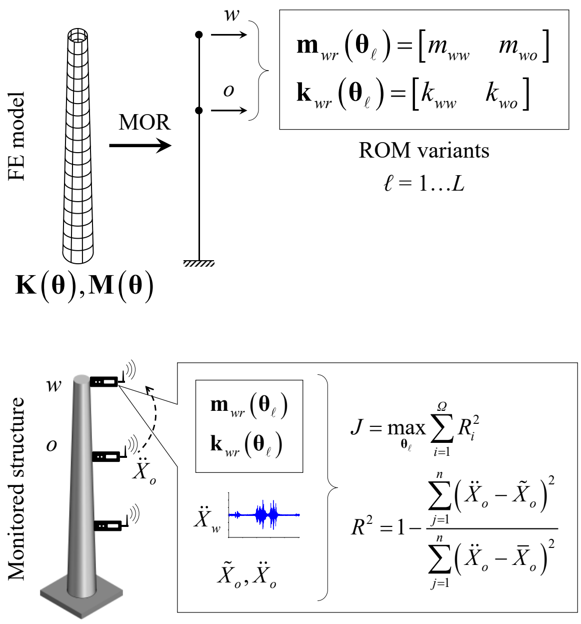

Figure 1: Overview of the decentralized digital twinning approach.

Implementation and validation

The prototypical implementation of the decentralized digital twinning approach involves the design of a relatively simple wireless SHM system, equipped with embedded physics-based models. In this section, first, the implementation details are illuminated, with emphasis on the software designed for the microcontrollers of the wireless sensor nodes. Thereupon, a small-scale laboratory test is presented, serving as proof of concept of the capability of the embedded physics-based models in identifying the structural condition.

Implementation in a prototype wireless SHM system

A key benefit of the decentralized digital twinning approach is the application of MOR in pairs of degrees of freedom, which allows a relatively minimal SHM system design, in terms of hardware. In fact, the proposed approach can be implemented even in SHM systems comprising only two wireless sensor nodes, one base station and one on-site computer (functioning as a server), as shown in Figure 2. The role of the base station and the on-site computer is secondary: The on-site computer is used for SHM system management (e.g. initialization, coordination) and data storage, and the base station acts as gateway node, enabling communication between the on-site computer and the wireless sensor nodes. Nevertheless, the wireless sensor nodes operate in a quasi-independent fashion, and the communication with the on-site computer is only performed when needed for system management and for transmitting data including results of the on-board computations for storage.

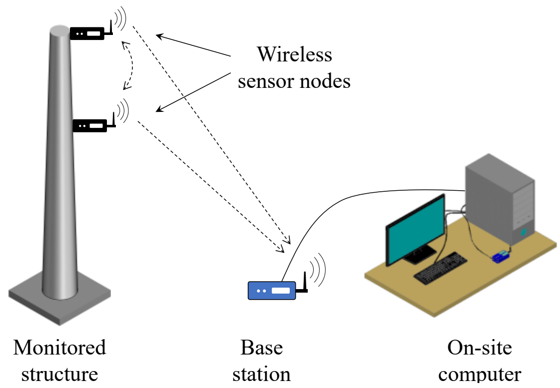

Figure 2: Layout of the prototype wireless structural health monitoring system.

Regarding the software implementation, embedded software for applying Equations 11 and 12 on board the wireless sensor nodes is exemplarily written in the Java programming language. The complexity of the software architecture is kept deliberately low to (i) preserve the limited computational resources of the sensor nodes and (ii) to facilitate the reproducibility of the code in other programming languages. An extract of the embedded software is shown in Figure 3.

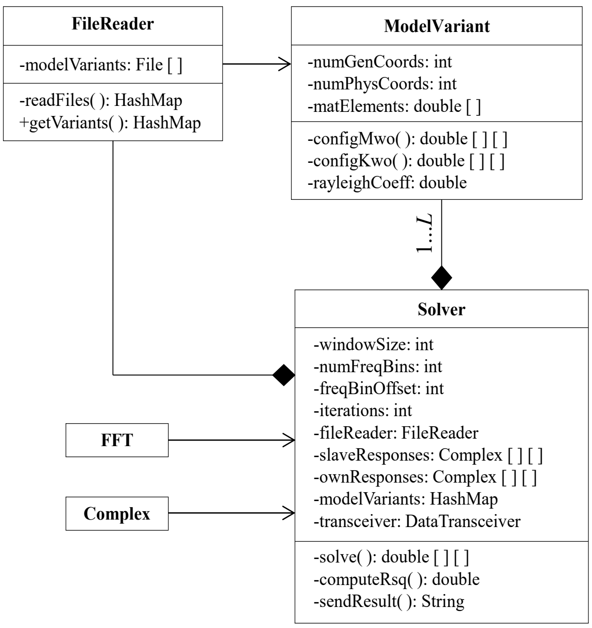

Figure 3: Extract of the embedded software.

The class `ModelVariant` realizes every reduced-order model variant, representing a damage scenario, the specifications of which are read as input streams by the `FileReader` class. Upon retrieving the responses $\ddot{\mathbf{X}}_w$ (`ownResponses` attribute) and the slave-DOF acceleration response data $\ddot{\mathbf{X}}_o$, the class `Solver` computes the estimates $\tilde{\mathbf{X}}_o$, using the method "`solve`" and the coefficient of determination for each model variant using the method "`computeRsq`". The outcome of the `Solver` class is communicated to the base station by invoking the method "`sendResult`". Finally, the FFT transform and the mathematical operations involving complex numbers are handled by the helper classes `FFT` and `Complex`, respectively. The prototype wireless SHM system is validated in a laboratory test, shown in the next subsection.

Validation test

The laboratory structure used for the validation test is shown in Figure 4. A 3-story shear-frame structure is employed, consisting of high-density-fiber (HDF) plates supported by aluminum columns. The density of the materials is assumed equal to 0.634 t/m^3 for the HDF and 2.70 t/m^3 for the aluminum, respectively. The elastic moduli are assumed equal to 3 MPa for the HDF and 70 MPa for the aluminum. Plate-to-column connections are fixed using two M3 screws per column. The dimensions of each plate are 300×200 (mm) (length × width) with a thickness of 18 mm and vertical inter-story spacing of 245 mm. The nominal cross-section dimensions of the columns are equal to 20×1.8 (mm) (width × thickness); however, the thickness of the columns is selected as "uncertain parameter" with high sensitivity and is used for calibrating the FE model. The column thicknesses, computed via model updating and used for MOR, are t_{z1} = 1.64 mm, t_{z2} = 1.79 mm and t_{z3} = 1.88 mm, for the first, second, and third story, respectively. At the base, the shear-frame structure is fixed on a 20-mm thick steel plate, which secures adequate clamping.

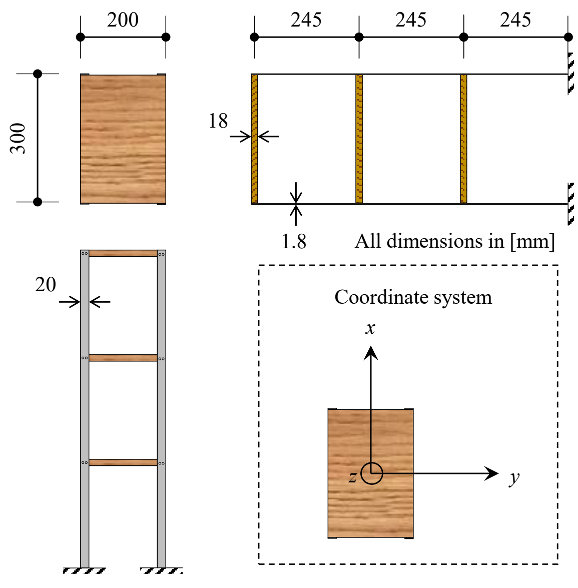

Figure 4: Laboratory shear-frame structure.

Two wireless sensor nodes are placed on the structure of type Oracle SunSPOT (Oracle Corp., 2010), featuring Java-based microcontrollers that enable the straightforward embedment of user-defined code. The software, presented in the previous subsection is embedded in the wireless sensor nodes, which are equipped with 3-axial accelerometers, capable of collecting acceleration response data at a sampling rate of 125 Hz, digitized with 8-bit resolution for a measurement range of ±2g. Despite the user-friendly interface of the SunSPOT wireless sensor nodes for embedding software, preliminary tests have revealed measurement inaccuracies, due to the low resolution of the accelerometer and the relatively high noise floor. To overcome the measurement inaccuracies, while leveraging the embedment capabilities of the SunSPOT sensor nodes, external measurement datasets are collected for each test case using high-accuracy wireless sensor nodes of type Lord Microstrain G-Link-200 (Parker Hannifin Microstrain Sensing, 2020). The external measurement datasets are subsequently deployed to the SunSPOT sensor nodes and used for applying the decentralized digital twinning approach.

The two wireless sensor nodes are placed on the first and second story, respectively, i.e. at heights of z_1 = 245 mm and z_2 = 450 mm. The sampling rate for the external measurement datasets is set equal to f_s = 128 Hz, and the measurement duration is 300 s for each test case. A window size of 2048 measurements is selected, resulting in n = 36 time windows with 50% overlap. Three test cases are considered: (i) undamaged ("intact") structure, (ii) minor damage, and (iii) major damage. For inflicting damage on the structure, the screws at the base of one column are loosened (one screw for "minor" damage and both screws for "major" damage). A family of L = 9 FE model variants are considered, including one FE model for the undamaged structure and 8 FE model variants, representing 4 different levels of damage per story for the bottom two stories. It should be noted that damage scenarios at the top story are not considered in this study, due to the negligible effect of top-story stiffness changes on the MOR of the FE model to the degrees of freedom of the bottom two stories. Following typical assumptions for shear-frame structure, the laboratory structure is modeled as a multi-DOF oscillator with one translational DOF per story in the x-axis direction. The translation in the y-axis direction is neglected due to the relatively high stiffness. Damage is simulated as stiffness reduction factors (0.9, 0.8, 0.7, 0.6) multiplied by the collective story stiffness ($4 \cdot k_c$, where k_c is the column stiffness). For selecting the range Ω of frequency components, the highest peaks in the FFT amplitude spectrum are located in each set of external measurements, and an offset of ±1 Hz is considered around each peak. The FFT amplitude spectra for the test cases (i) and (iii) are exemplarily illustrated in Figures 5 and 6. As can be seen in the FFT amplitude spectra, the effect of damage is relatively small in the second and third peak, leading to the conclusion that extending the range to include these peaks may be hardly sensitive to the damage scenario considered and are, therefore, excluded from Ω. All test cases are conducted by hammer-induced excitation. The results are summarized in Table 1.

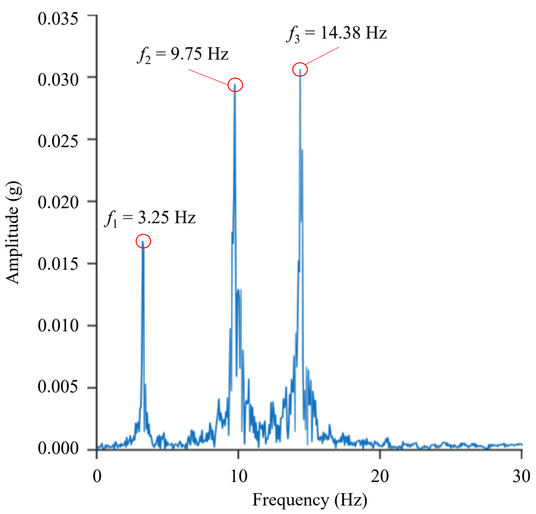

Figure 5: FFT amplitude spectrum for test case (i) (intact structure).

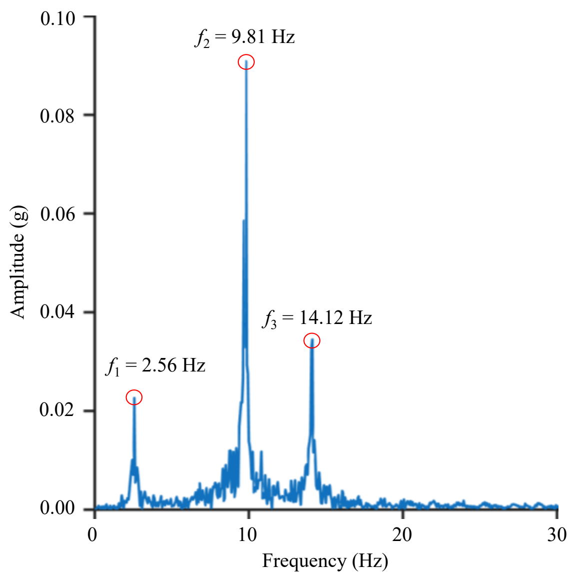

Figure 6: FFT amplitude spectrum for test case (iii) (major damage).

Table 1: $\sum R^2$ for all test cases and all model variants.

Model variant	Stiffness reduction factor	Test case (i)	Test case (ii)	Test case (iii)
Intact	N/A	**58.86**	56.33	53.00
Damage on 1st story	0.9	58.67	56.79	54.71
	0.8	58.20	**56.91**	55.96
	0.7	57.46	56.69	56.77
	0.6	56.43	56.12	**57.13**
Damage on 2nd story	0.9	58.77	55.63	51.27
	0.8	58.37	54.41	48.64
	0.7	57.37	52.27	44.53
	0.6	55.23	48.40	37.75

The test results clearly show that the decentralized digital twinning approach yields the fittest model variant most compatible with the test case considered. In test case (i), the “intact” model variant receives the highest R^2 value, although the proximity with model variants representing minor damage is close, indicating the sensitivity of the approach to measurement inaccuracies. The fittest model variant for test case (ii) is the model with reduction factor 0.8 at the first story, which is expected, since the damage inflicted is minor. By contrast, the fitness of the significant-damage model variant with reduction factor 0.6 is prominent in test case (iii), where damage is indeed major. Nevertheless, the applicability of the decentralized digital twinning approach needs to be investigated in large-scale experiments, which will be covered in future work.

Summary and conclusions

Embedded computing has been employed in wireless structural health monitoring as a means of reducing the power-consuming transmission of large sets of structural response data. However, most embedded computing approaches rely on data-driven analysis, which yields limited information on the structural condition, due to the implicit consideration of the physics dominating the structural behavior. This paper has reported on embedding physics-based models for conducting SHM tasks directly on wireless sensor nodes, realized as decentralized digital twins. The proposed decentralized digital twinning approach relies on model-order reduction (to render the physics-based models – in practice, finite element models – computationally manageable by the sensor nodes) and model segmentation (to enable wireless sensor nodes to use the models quasi-independently). The decentralized digital twinning approach has been implemented in a prototype wireless SHM system and validated in a small-scale laboratory test, serving as proof of concept for the capability of the approach to correctly identify structural damage. Future work will focus on investigating the applicability limits of the decentralized digital twinning approach, via large-scale tests on real-world structures.

Acknowledgments

The authors gratefully acknowledge the support offered by the German Research Foundation (DFG) through grants SM 281/9-3, SM 281/33-1 and SM 281/44-1, as well as by the German Federal Ministry of Transport (BMV) under grant 01FV2059C. Any opinions, findings, conclusions, or recommendations expressed in this paper are those of the authors and do not necessarily reflect the views of the DFG.

References

Al-Zuriqat, T., Chillón Geck, C., Dragos, K., Manolis, G. D., & Smarsly, K. (2025). Decentralized sensor fault diagnosis for wireless structural health monitoring systems using Artificial Intelligence of Things. In: 15th International Workshop on Structural Health Monitoring (IWSHM). Stanford, CA, USA, 09/11/2025.

Avci, O., Abdeljaber, O., Kiranyaz, S., Hussein, M., and Inman, D.J. (2018). Wireless and real-time structural damage detection: A novel decentralized method for wireless sensor networks. Journal of Sound and Vibration, 424, pp. 158-172.

Bathe, K.-J. and Dong, J. (2014). Component mode synthesis with subspace iterations for controlled accuracy of frequency and mode shape solutions. Computers and Structures, 139, pp. 28-32.

Buckley, T., Ghosh, B., and Pakrashi, V. (2021). Edge structural health monitoring (E-SHM) using low-power wireless sensing. Sensors, 21, 20, ID: 6760.

Çelebi, M. (2002). Seismic instrumentation of buildings (with emphasis on federal buildings). Technical report No. 0-7460-68170. Menlo Park, CA, USA: United States Geological Survey.

Dragos, K. and Smarsly, K. (2015). A comparative review of wireless sensor nodes for structural health monitoring. In: 7th International Conference on Structural Health Monitoring of Intelligent Infrastructure. Turin, Italy, 07/01/2015.

Dragos, K. and Smarsly, K. (2016). Distributed adaptive diagnosis of sensor faults using structural response data. Smart Materials and Structures, 25, 10, ID: 105019.

Dragos, K. and Smarsly, K. (2017). Decentralized infrastructure health monitoring using embedded computing in wireless sensor networks. In: Sextos, A. & Manolis, G. D. (eds.). Dynamic Response of Infrastructure to Environmentally Induced Loads. Pp. 183-201. Cham, Switzerland: Springer International Publishing AG.

Dragos, K. and Smarsly, K. (2024). A smart monitoring approach based on decentralized digital twins. In: 20th International Conference on Computing in Civil and Building Engineering (ICCCBE). Montréal, Canada, 08/25/2024.

Dragos, K., Theiler, M., Magalhães, F., Moutinho, C., and Smarsly, K. (2018). On-board data synchronization in wireless structural health monitoring systems based on phase locking. Structural Control and Health Monitoring, 25, 11, ID: e2248.

Friedmann, A., Mayer, D., and Kauba, M. (2010). An approach for decentralized mode estimation based on the random decrement method. Shock and Vibration, 17, 4-5, pp. 579-588.

Fritz, H., Peralta, J., Legatiuk, D., Steiner, M., Dragos, K., and Smarsly, K. (2022). Fault diagnosis in structural health monitoring systems using signal processing and machine learning techniques. In: Cury, A., Ribeiro, D., Ubertini, F., Todd, M. D. (eds.). Structural health monitoring based on data science techniques. Pp. 143-164.

Kijewski-Correa, T. and Su, S. (2009). BRAIN: A bivariate data-driven approach to damage detection in multi-scale wireless sensor networks. Smart Structures and Systems, 5, 4, pp. 415-426.

Mitchel, K., Sana, S., Liu, P., Cingirikonda, K., Rao, V.S., and Pottinger, H.J. (2000). Distributed computing and sensing for structural health monitoring systems. In: SPIE Smart Structures and Materials: Smart Electronics and MEMS. Newport Beach, CA, USA: 03/06/2000.

Nagayama, T., Spencer Jr, B.F., and Rice, J.A. (2009). Autonomous decentralized structural health monitoring using smart sensors. Structural Control Health Monitoring, 16, 7-8, pp. 842-859.

Lynch, J.P. and Loh, K.J. (2006). A summary review of wireless sensor networks for structural health monitoring. The Shock and Vibration Digest, 38, 2, pp. 91-128.

Lynch, J.P., Sundararajan, A., Law, K.H., Kiremidjian, A.S., and Carryer, E. (2004). Embedding damage detection algorithms in a wireless sensing unit for operational power efficiency. Smart Materials and Structures, 13, 4, pp. 800-810.

Oracle Corp. (2010). Sun SPOT eDEMO Technical Datasheet, 8th edition. Santa Clara, CA, USA: Sun Labs.

Park, G., Rosing, T., Todd, M.D., Farrar, C.R., and Hodgkiss, W. (2008). Energy harvesting for structural health monitoring sensor networks. ASCE Journal of Infrastructure Systems, 14, 1, pp. 64-79.

Parker Hannifin Microstrain Sensing (2020). Microstrain Sensing Product Datasheet: G-Link-200 Ruggedized Wireless Triaxial Accelerometer Node. Williston, VT, USA: Parker Hannifin Corp.

Peckens, C.A., Lynch, J.P., and Pei, J.-S. (2011). Distributed neural computations for embedded sensor networks. In: SPIE Smart Structures and Materials: Nondestructive Evaluation and Health Monitoring. San Diego, CA, USA, 03/06/2011.

Quqa, S., Giordano, P.F., Limongelli, M.P., Landi, L., and Diotallevi, P.P. (2021). Clump interpolation error for the identification of damage using decentralized sensor networks. Smart Structures and Systems, 27, 2, pp. 351-363.

Smarsly, K. and Law, K.H. (2014). Decentralized fault detection and isolation in wireless structural health monitoring systems using analytical redundancy. Advances in Engineering Software, 73, pp. 1-10.

Spencer Jr., B.F. and Cho, S. (2011). Wireless smart sensor technology for monitoring civil infrastructure: Technological developments and full-scale applications. In: 2011 World Congress on Advances in Structural Engineering and Mechanics (ASEM 11). Seoul, S. Korea, 09/18/2011.

Spencer Jr, B.F., Ruiz-Sandoval, M.E., and Kurata, N. (2004). Smart sensing technology: Opportunities and challenges. Structural Control Health Monitoring, 11, pp. 349-368.

Wang, Y., Lynch, J.P., and Law, K.H. (2007). A wireless structural health monitoring system with multithreaded sensing devices: design and validation. Structure and Infrastructure Engineering, 3, 2, pp. 103-120.

Yi, X., Zhu, D., Wang, Y., Guo, J., and Lee, K.-M. (2010). Embedded transmissibility function analysis for damage detection in a mobile sensor network. In: SPIE Smart Structures and Materials: Nondestructive Evaluation and Health Monitoring. San Diego, CA, USA, 03/07/2010.

Zimmerman, A.T., Shiraishi, M., Swartz, R.A., and Lynch, J.P. (2008). Automated Modal Parameter Estimation by Parallel Processing within Wireless Monitoring Systems. ASCE Journal of Infrastructure Systems, 14, 1, pp. 102-113.